Two novel effectors of trafficking and maturation of the yeast plasma membrane H^+-ATPase

Running title: *Two novel effectors of Pma1 trafficking*

Key words: Ydl121c, Exp1, Ykl077w, Psg1, Pma1, COPI, COPII, Lst1, Sec24, Kex2.

Yosef Geva	Department of Molecular Genetics, Weizmann Institute of Science
Jonathan Crissman	Department of Biological Sciences, Columbia University
Eric C. Arakel	Department of Molecular Biology, Universitätsmedizin Göttingen
Natalia Gómez-Navarro	MRC Laboratory of Molecular Biology
Silvia G. Chuartzman	Department of Molecular Genetics, Weizmann Institute of Science
Kyle R. Stahmer	Department of Biological Sciences, Columbia University
Blanche Schwappach	Department of Molecular Biology, Universitätsmedizin Göttingen

corresponding authors

Maya Schuldiner

Department of Molecular Genetics, Weizmann Institute of Science.

Rehovot 7610001, Israel.

Ph. +972-8-934-6346

Fax. +972-8-934-6373

maya.schuldiner@weizmann.ac.il

Elizabeth A. Miller

MRC Laboratory of Molecular Biology.

Francis Crick Avenue, Cambridge CB2 0QH, UK.

Ph. +44 1223 267042

emiller@mrc-lmb.cam.ac.uk

Two novel effectors of trafficking and maturation of the yeast plasma membrane H^+-ATPase

Yosef Geva[1], Jonathan Crissman[2], Eric C. Arakel[3], Natalia Gómez-Navarro[4], Silvia G. Chuartzman[1], Kyle R. Stahmer[2], Blanche Schwappach[3], Elizabeth A. Miller[2,4] and Maya Schuldiner[1].

This article has been accepted for publication and undergone full peer review but has not been through the copyediting, typesetting, pagination and proofreading process, which may lead to differences between this version and the Version of Record. Please cite this article as doi: 10.1111/tra.12503

1. Department of Molecular Genetics, Weizmann Institute of Science, Rehovot 7610001, Israel.

2. Department of Biological Sciences, Columbia University, New York 10027, USA.

3. Department of Molecular Biology, Universitätsmedizin Göttingen, Humboldtallee 23, Göttingen 37073, Germany.

4. MRC Laboratory of Molecular Biology, Francis Crick Avenue, Cambridge CB2 0QH, UK

Correspondence:

emiller@mrc-lmb.cam.ac.uk; maya.schuldiner@weizmann.ac.il

ABSTRACT

The endoplasmic reticulum (ER) is the entry site of proteins into the endomembrane system. Proteins exit the ER via COPII vesicles in a selective manner, mediated either by direct interaction with the COPII coat or aided by cargo receptors. Despite the fundamental role of such receptors in protein sorting, only a few have been identified. To further define the machinery that packages secretory cargo and targets proteins from the ER to Golgi membranes, we used multiple systematic approaches, which revealed two uncharacterized proteins that mediate the trafficking and maturation of Pma1, the essential yeast plasma membrane proton ATPase. Ydl121c (Exp1) is an ER protein that binds Pma1, is packaged into COPII vesicles, and whose deletion causes ER retention of Pma1. Ykl077w (Psg1) physically interacts with Exp1 and can be found in the Golgi and COPI vesicles but does not directly bind Pma1. Loss of Psg1 causes enhanced degradation of Pma1 in the vacuole. Our findings suggest that Exp1 is a Pma1 cargo receptor and that Psg1 aids Pma1 maturation in the Golgi or affects its retrieval. More generally our work demonstrates the utility of high content screens in the identification of novel trafficking components.

INTRODUCTION

The endoplasmic reticulum (ER) is the entry site for proteins into the endomembrane system. Once appropriately folded, non-ER resident proteins are routed to the Golgi apparatus for further maturation and distribution[1]. Proteins exit the ER via COPII vesicles. Although some proteins are captured by stochastic sampling of the ER lumen and membrane in a process called bulk flow[2,3], more efficient and regulated sorting relies on selective uptake into vesicles. Additional sorting specificity occurs by retrieval of ER residents or immature proteins from the Golgi apparatus to the ER through COPI vesicles[4,5].The general mechanisms of vesicle formation are well characterized, yet the molecular basis that governs specific recognition between the coats, and the diverse range of proteins that must be packaged into vesicles, is yet to be fully described.

The cargo binding subunit in the COPII coat is Sec24. One of the characteristics of Sec24 that enables it to bind many diverse cargoes is the presence of three isoforms: Sec24, Iss1 (Sfb2) and Lst1 (Sfb3), each with multiple distinct binding sites for cargo or adaptors[6–8]. Each Sec24 isoform will yield COPII vesicles that differ in their cargo and lipid content[9,10]. For example, the Lst1 isoform is necessary for efficient traffic of some GPI-anchored proteins[11] and Pma1, the plasma membrane H^+-ATPase[12], two classes of proteins that reside in sterol and ceramide/ sphingolipid rich domains[13].

Importantly, although combinatorial use of Sec24 isoforms increases binding opportunities, this is unlikely to account for the full spectrum of cargo diversity handled by the COPII system. Additional diversity stems from the use of cargo receptors, whose role is to bind cargo and indirectly connect it to a specific binding site of a Sec24 family protein[14–21] Some cargo receptors further increase the diversity of their cargo capture by binding additional adaptors[22–24]. Finally, additional modes of Sec24 interaction can also increase diversity and specificity: some cargoes are capable of binding two separate sites[6]; others bind cooperatively through both direct Sec24 interaction and indirect receptor-mediated interaction[8].

Currently, there are around 15 known cargo receptors in the budding yeast, *Saccharomyces cerevisiae*[5]. Taking into consideration the hundreds of proteins that must be effectively sorted into COPI or COPII vesicles at any given moment, even in the simplest eukaryotic model organism, yeast, the existence of additional cargo receptors and adaptors is postulated. Here, we used mutations in the binding sites of yeast Sec24 to perturb ER to Golgi traffic in the context of more than 374 individually tagged yeast proteins targeted to the secretory pathway. This approach coupled with a high-content microscopic screen revealed a novel cargo receptor for the essential yeast plasma membrane H^+-ATPase, Pma1.

RESULTS

A high-content screen uncovers an uncharacterized protein that cycles between the ER and the Golgi apparatus

To better understand the regulation of protein flux through the secretory pathway, we aimed to define new cargo receptors. One of the hallmarks of a cargo receptor is that it dynamically cycles through the ER and Golgi via COPII and COPI vesicles. However, cargo receptors are not usually visualized in all these compartments in parallel but tend to hold a single, typical, steady state localization. We hypothesized that by perturbing the ER-Golgi cycle we could capture cargo receptors in a stereotypical way that would allow us to identify novel candidate receptors. To this end, we visualized a large number of secretory pathway proteins tagged with Green Fluorescent Protein (GFP) on the background of perturbed ER-Golgi traffic. Specifically we selected 374 strains each expressing a protein that resides in the secretory pathway that is genomically tagged with GFP at its C terminus[25]. This "secretome library" encompasses proteins localized to either the ER, Golgi apparatus, plasma membrane, vacuolar membrane, vacuolar lumen, COPI or COPII vesicles, peroxisomes, undefined punctate localization and secreted proteins[19].

To perturb traffic we chose to use mutations in the cargo binding sites of Sec24 as it was already shown that a mutation in the Sec24-A binding site perturbs ER-Golgi vesicular traffic[26]. Moreover, the two best-characterized cargo of the A- and C-sites are SNARE proteins that act in anterograde (Sed5) and retrograde (Sec22) traffic, suggesting that bidirectional traffic between the ER and Golgi would be perturbed in these mutants. In contrast, many cargo that engage the B-site are proteins that move forward in the secretory pathway. Thus we focused on A- and C-site mutations that should more specifically perturb ER-Golgi vesicular traffic[6,7]. We used automated mating techniques to integrate these Sec24 binding site mutants into the secretome-GFP library[27] and imaged the resulting strains using a high content setup[28].

Manual examination of the resulting images revealed that A- and C-site mutations altered the localization of only a handful of proteins, the majority of which were known cargo receptors as expected. Four members of the p24 family, Erp1, Erp2, Erp4, and Erv25, were redistributed from the ER to an ER/punctate localization on the background of mutation in the Sec24 C-site (Fig. 1B). Three proteins showed altered localization in both A- and C-site mutants: two known cargo receptors, Erv41 and Erd2, and a putative ER protein with unknown function, Ydl121c (Fig. 1C). Erd2 is the retrieval receptor of HDEL bearing proteins and Erv41 is a retrieval receptor of Gls1, Fpr2 and other non-HDEL bearing proteins[29,30]. We therefore hypothesized that Ydl121c may also be a cargo receptor. Indeed, co-localization studies revealed that on the background of Sec24 mutants, Ydl121c-GFP moved from an ER localization to being co-localized with the COPI marker, Cop1-mCherry (Fig. S1).

Ydl121c interacts genetically and physically with Pma1.

Ydl121c is a small, type I, membrane protein of 149 amino acids (aa), harboring a single transmembrane domain (TMD) with only 6 N-terminal aa facing the ER lumen and a cytosolic domain of 123 aa (Fig. 2A)[31,32]. If indeed Ydl121c has a role in ER to Golgi traffic it should bud from the ER in COPII vesicles. To test this we used an *in vitro* budding assay, which showed that indeed HA-tagged Ydl121c is actively packaged into COPII vesicles (Fig. 2B).

To test if Ydl121c is a cargo receptor we sought to identify potential cargo. We first searched for physically interacting partners by immunoprecipitation of HA-tagged Ydl121c followed by mass spectrometry. Mass spectrometry identified eleven reproducible, high-confidence interactors (Fig. 2C). Seven of the interactors reside in the endomembrane system, including four subunits of the auxiliary ER translocation channel (Sec72, Snd3, Sss1, Sec63)[33,34] and one component of COPI vesicles (Sec28) and of COPII vesicles (Erv14). While their specific relevance remains to be investigated, these interactors are consistent with the ER residence of Ydl121c and may reflect its cycling in the early secretory pathway. Of the endomembrane system proteins, only Pma1 was an interactor that is not resident in the early secretory pathway. Since Pma1 was enriched as much as Ydl121c itself in the pull-downs, we considered Pma1 a candidate cargo client for Ydl121c.

In parallel to uncovering its physical interaction partners, we explored the genetic interactions of Δ*ydl121c* using a synthetic lethality screen. We crossed a Δ*ydl121c* query strain with the yeast haploid deletion and hypomorphic (DAmP) collections[35,36]. Of particular interest among the small number of synthetic lethal interactors were *Δlst1,* the Sec24 homolog that promotes efficient ER exit of Pma1, and *Δbrp1,* a deletion of a dubious open reading frame that leads to down-regulation of *PMA1*[37,38] (Table S4). To verify these interactions, we performed a manual cross between a strain carrying the Δ*ydl121c* allele and one carrying a Δ*lst1* allele. Following meiosis we used tetrad dissection to isolate progeny. Consistent with the systematic screen results, we could not recover viable spores that bore both Δ*ydl121* and Δ*lst1,* confirming a synthetic lethal interaction between these genes (Fig. 2D). The finding that deletion of these two genes - a major regulator of Pma1 trafficking and a hypomorphic allele of *PMA1* - causes synthetic lethality with Δ*ydl121* implies that in cases of perturbed trafficking or synthesis of Pma1, Ydl121c becomes essential. These results support our hypothesis that Pma1 is a client of the candidate cargo receptor Ydl121c.

Pma1 is an abundant and essential yeast plasma membrane protein that functions as a H^+-ATPase[39]. This 100 kDa protein contains 10 TMDs and oligomerizes into dodecamers during its synthesis in the ER[12,40]. Given its abundance and essentiality, it is perhaps not surprising that Pma1 requires efficient and tightly controlled mechanisms of ER exit and accessory factors to promote its biogenesis and traffic.

Ydl121c is a specific cargo receptor for Pma1

The Sec24 subunit that affects Pma1 trafficking the most, Lst1 (*lethal with sec-thirteen)*, was originally identified through its synthetic lethal interaction with the COPII coat component, Sec13. If Ydl121c is similarly required for efficient ER export of Pma1, we reasoned that it might also be lethal with the temperature-sensitive (ts) *sec13-1* allele. Indeed when *Δydl121* or *Δlst1* mutations were introduced into the *sec13-1* strain, they were both synthetic lethal even at the permissive temperature of 28ºC (Fig. 3A). Moreover, overexpression of *YDL121C* could rescue the lethal phenotype of *sec13-1/Δlst1*. The fact that *LST1* and *YDL121C* show similar interaction with *sec13-1* and the capability of *YDL121C* O.E to overcome *LST1* loss strongly suggest a parallel role for these two proteins. In addition, overexpression of *YDL121C* could rescue loss of *lst1* at pH=2.5, a condition that would require efficient Pma1 export, to the same level as *LST1* itself (Fig 3B). Again showing that Ydl121c can facilitate Pma1 trafficking independently of Lst1 at least to some extent.

We next asked whether Ydl121c is specific to Pma1 or may be required for the packaging of other Lst1-dependent cargoes, such as GPI-anchored proteins (GPI-APs). We therefore examined the maturation of the GPI-AP, Gas1, using pulse-chase analysis, where export from the ER and delivery to the Golgi causes a shift in molecular weight from the precursor (p) to mature (m) form that can be readily quantified. Whereas Gas1 maturation was significantly slowed in a Δ*lst1* strain relative to wild-type, the Δ*ydl121c* strain showed no such defect (Fig. 3C). This suggests that Ydl121c is a specific cargo receptor for Pma1 and does not participate in Lst1-dependent GPI-AP trafficking.

Ydl121c and Ykl077w may work together to promote efficient Pma1 maturation.

To further characterize Ydl121c function, we searched again for potential interactors, using this time an *in vivo* protein interaction assay that works by split DiHydro Folate Reductase complementation (Split DHFR screen)[41]. The strongest interaction that we detected was with an uncharacterized protein, Ykl077w. *YKL077W* encodes an open reading frame that should give rise to a 392aa protein with a predicted signal sequence at its N-terminus and a single transmembrane domain near the C-terminus. The short cytosolic region bears two putative retrieval motifs KRR and KKxxKxx (Fig. 4A). Interestingly, Ykl077w was previously shown to be cleaved by the Ca^+ dependent serine protease, Kex2. This cleavage was shown to give rise to a ~30kDa transmembrane protein[42] when the C' portion was followed. However, it was not determined whether the N' portion also gives rise to a stable fragment or whether it is only necessary for the biogenesis of Ykl077w. To follow the N' fragment we N' tagged Ykl077w and found that indeed, the N' itself also gives rise to a mature protein (Fig. 4B). Apparently this phenomenon is common to other Kex2 substrates as well[43]. The full-length form of the protein is short lived and can only be detected on the background of *Δkex2*. Interestingly, Ykl077w-N' runs at a much higher molecular weight than would be predicted by its length, suggesting that it is highly glycosylated (Fig. 4B). In support of this, many sites on Ykl077w-N' were recently shown to be O-mannosylated in a high throughput analysis of glycosylation in yeast[44] (Fig. S2). We performed pull downs of Ykl077w-N' and Ykl077w-C', which demonstrated physical interactions with most of the Golgi glycosylation machinery (Tables S5+S6). Existing genetic interaction data indeed shows that the glycosylation complex and *ykl077w* have a buffering interaction suggesting a co-dependence[45]. Both Ykl077w-N' and Ykl077w-C' showed significant enrichment for a physical interaction with Ydl121c (Tables S5+S6). In contrast to Ydl121c, neither Ykl077w N' nor C' showed a physical interaction with Pma1.

To see whether the two Ykl077w derived proteins function in the same cellular compartment we co-localized GFP-Ykl077w and Ykl077w-GFP with a variety of markers for the endomembrane system and found that while the full length or Ykl077w-N' is mostly co-localized with the ER and mid-Golgi (Fig. 4C), the Ykl077w-C' is mostly co-localized with COPI vesicles although some co-localization was seen with Golgi markers as well (Fig. 4D). The fact that each fragment has a different steady-state localization should be taken into consideration when attempting to understand the role of Ykl077w in sorting or maturation in the early secretory pathway.

Loss of Ykl121c or Ykl077w affects Pma1 maturation.

To assess the direct influence of Ydl121c and Ykl077w on Pma1 we quantified untagged, endogenous, Pma1 levels. The Δ*ydl121c* strain showed a 20% reduction in Pma1 abundance relative to the WT control and the Δ*ykl077w* strain showed a reduction of more than 80% in Pma1 abundance (Fig. 5A).

One key feature of Pma1 biogenesis is its assembly into larger multimers, which occurs during early stages of maturation within the ER[40,46]. We therefore tested the abundance and assembly of Pma1 under native conditions using blue native gel electrophoresis. In all strains we could readily detect the fully assembled

complex as well as several intermediate complexes of Pma1, however both Δ*ydl121c* and Δ*ykl077w* strains showed a reduction of Pma1 abundance in all forms (Fig. 5B).

To visualize the cellular compartment in which Pma1 is most affected, we introduced Pma1 C-terminally tagged with GFP (Pma1-GFP) on the background of Δ*ydl121c* or Δ*ykl077w*. During continuous logarithmic growth, when Pma1-GFP is normally localized to the plasma membrane and vacuole (Fig. 5C), loss of Ydl121c caused an ER retention phenotype and loss of Ykl077w caused accumulation in the vacuole lumen (Fig. 5C), which could explain the reduced abundance of Pma1 in this background. Indeed, measurement of free GFP, which is stable in the vacuole lumen [47] demonstrates that Δ*ykl077w* accumulates free GFP (Fig. 5D). Taken together, our data suggests that Ydl121c and Ykl077w both contribute to Pma1 maturation and sorting albeit in different ways.

DISCUSSION

Pma1, the yeast H+-ATPase and the major regulator of cytoplasmic pH and plasma membrane potential, is the most abundant protein in the plasma membrane[39]. Pma1 maturation is highly complex as it oligomerizes to hexamers and dodecamers within the ER in a manner dependent on ceramide biosynthesis. Its traffic relies on incorporation into ER-derived vesicles most likely enriched in sterols and sphingolipids, and harboring the Sec24 homolog Lst1[12,40]. Its further trafficking from the Golgi to the plasma membrane is aided by two additional proteins, Ast1 and Ast2, that stabilize it in ceramide-rich domains in the membrane[48,49]. While searching for proteins that take part in ER-to-Golgi traffic we found two novel, uncharacterized proteins that seem to promote and regulate the sorting of Pma1: Ydl121c that has been named Exp1 (for ER eXport of Pma1, Chris Kaiser and Darcy Morse, personal communication) and Ykl077w that we now name Psg1 (Pma1 Stabilization in the Golgi).

Our experiments suggest that Exp1 is a cargo receptor for Pma1 to exit the ER. First, just like other cargo receptors it cycles between the ER and Golgi and is affected by Sec24 cargo-binding site mutants. In support of our findings, Exp1 was found to be enriched in COPI/COPII vesicles in two independent studies[24,50] and we found that it is packaged into COPII vesicles *in vitro*. Second, Exp1 physically binds Pma1 as would be expected for a cargo receptor. Exp1 also binds several ER translocation channel components raising the intriguing possibility that it binds Pma1 soon after translocation and escorts it to exit sites. Third, *Δexp1* shows synthetic lethality with a hypomorphic allele of *PMA1* and with *Δlst1*, the *SEC24* homolog dedicated to Pma1 export from the ER. These genetic interactions are consistent with a functional role in increasing the rate or fidelity of ER export of a specific substrate. Finally, loss of Exp1 causes ER retention of Pma1-GFP and reduced steady-state levels of all multimeric forms of the protein. We would therefore hypothesize that Exp1 works to package Pma1 into Sec24 containing vesicles in a manner that is parallel to Lst1 (Fig. 6).

The function of Psg1 is less clear. We showed that Psg1, cleaved by the Ca^{+} dependent serine protease Kex2, gives rise to two stable cleavage products that we now name Psg1-N' and Psg1-C' (Fig. 6). Our experiments do not differentiate which of the two product of Psg1 affect Pma1 trafficking as all of our genetic ablations remove both isoforms. It remains to be determined in the future whether the two proteins act together or separately to facilitate Pma1 maturation and if the short-lived, full-length, protein form is also active. Moreover, we could not detect a physical interaction between Psg1 and Pma1 suggesting that its mode of action is indirect. However, losing Psg1 caused increased vacuolar accumulation of Pma1-GFP and dramatically reduced Pma1 levels. This could be due to faulty sorting of the protein to the vacuole instead of to the plasma membrane or as a consequence of increased endocytosis. It may also be that Psg1 has a role in ER retrieval of escaped Pma1 monomers that are immature or misassembled that have escaped the ER to give them another chance of assembly, and in its absence, Golgi quality control mechanisms route the monomer to the vacuole[51].

Interestingly the N' tagged Psg1 showed physical interactions with ERAD-related proteins involved in Pma1 quality control (Eps1, Cdc48, Ubx2, Ssm4) (Table S5)[52] supporting a role in maturation quality control for this protein. The C' Psg1 demonstrated physical and genetic interaction with the Tlg1/2 SNARE complex (Tlg1, Tlg2, Vti1) (Table S6) suggesting a role in modulating vesicular trafficking. Psg1 was also found to be associated with Golgi mannosyl transferase complexes and exhibits a genetic profile correlative with being associated with the glycosylation pathway[45], hence Psg1 might couple Pma1 sorting and maturation in the early secretory pathway with the glycosylation machinery. In validation of this, we found that deletion of *MNN11*, one of the Golgi mannosyl transferase subunits caused enhanced vacuolar degradation of Pma1 similar to the deletion of *PSG1.* However double deletion of *PSG1, MNN11* had a suppressor effect and completely abolished the vacuolar degradation phenotype (Fig. S3).

Since Δ*psg1* and Δ*exp1* did not show a negative genetic interaction with each other but were found to physically interact, we hypothesize that they act sequentially to promote Pma1 sorting between the ER and the Golgi. It can be suggested that Exp1 promotes Pma1 export from the ER to the Golgi while Psg1 has a role in Pma1 maturation or quality control in the Golgi (Fig. 6). More generally, our screening strategy allowed us to identify two novel players in

ER-Golgi traffic regulating, one of the most important and abundant proteins in the cell.

MATERIALS AND METHODS

Yeast strains and strain construction

All yeast strains in this study are based on the BY4741 laboratory strain[53]. Manipulations were performed using a standard PEG/LiAC transformation protocol[54]. Deletions were verified using primers from within the endogenous open reading frame. Primers for all genetic manipulations were planned by Primers-4-Yeast web tool[55]. All strains and plasmids used in this study are listed (Table S1 and S2). To construct the Secretome GFP library, we initially chose 565 strains that represent a variety of secretory pathway proteins from the C'-tagged GFP library[25] To assemble the library, we hand-picked all possible secretory pathway proteins. The initial array was visualized and only 374 strains displaying a strong and correctly localized GFP signal were put into the final array (a full list of selected strains is available in Table S3).

The *sec13-1* double mutant strains were made by transforming the parental *sec13-1* strain (RSY2069/LMY282) containing a *SEC13-URA3* plasmid (pLM246) with a PCR-amplified deletion cassette with overlap to the *LST1* locus (pAG25[56]). The *sec13-1 exp1::HPHMX4* double mutant strain was made similarly using a deletion cassette (pAG32[56]) and *EXP1* locus overlap.

Yeast media and growth conditions

Cultures were grown at 30°C in either rich medium [1% Bacto-yeast extract (BD), 2% Bacto-peptone (BD) and 2% dextrose (Amresco)] or synthetic medium [0.67% yeast nitrogen base with ammonium sulfate and without aa (CondaPronadisa) and 2% dextrose (Amresco), containing the appropriate supplements for plasmid selection][57]. When needed as selection markers, G418 (200µg/ml, Calbiochem) or Nourseothricin (Nat) (200µg/ml WERNER BioAgents) were added. In cases where G418 was required in a synthetic medium, yeast nitrogen base without ammonium sulfate (CondaPronadisa) was added and supplemented with monosodium glutamate (Sigma) as an alternative nitrogen source.

For dilution assay strains were grown to saturation and 1:10 serial dilutions were plated on agarose media containing 5-FOA to counterselect for the *SEC13-URA3* plasmid. Plates were incubated at the indicated temperatures for 2 days before imaging.

Pulse-Chase Analysis

Maturation of Gas1 was monitored by pulse-chase analysis as described in[58].

Protein structure prediction

Prediction of protein architecture was performed using Protter[32].

Automated yeast library manipulations and high-throughput microscopy

Automated mating procedures and microscopic screening were performed using an automated microscopy set-up as previously described[27,28], using the RoToR bench-top colony arrayer (Singer Instruments) and automated inverted fluorescent microscopic ScanR system (Olympus). Images were acquired using a 60X air lens with excitation at 490/20 nm and emission at 535/50 nm (GFP) or excitation at 575/35 nm and emission at 632/60 nm (mCherry/RFP). After acquisition, images were manually reviewed using the ScanR analysis program.

Manual microscopy

Manual microscopy was performed using the VisiScope Confocal Cell Explorer system, composed of a Zeiss Yokogawa spinning-disk scanning unit (CSU-W1) coupled with an inverted Olympus IX83 microscope. Images were acquired using a 60X oil lens and captured by a connected PCO-Edge sCMOS camera, controlled by VisView software, with wavelength of 488nm (GFP) or 561nm (mCherry/RFP). Images were transferred to ImageJ for slight contrast and brightness adjustments.

In vitro budding into COPII vesicles.

Microsomal membranes were prepared from yeast cells expressing HA-tagged Ydl121c and used for in vitro vesicle formation as described[7]. In brief, membranes were washed with urea to remove endogenous COPII proteins, then incubated with purified Sar1, Sec23/Sec24 and Sec13/Sec31 in the presence of GDP (negative control) or GTP plus an ATP regeneration system. Vesicles were separated from donor membranes by medium speed centrifugation (12,000 rpm) and the vesicle fraction collected by high speed centrifugation (100,000 x g). A fraction of the total donor membranes (T) and the vesicle fractions were analyzed by immunoblotting.

Affinity purification and mass spectrometry

Yeast cells expressing HA tagged Exp1 at the N' or C' or GFP tagged Psg1 N' or C' were harvested from mid-logarithmic growth phase. Cells were snap frozen in liquid nitrogen and ground (CryoMill, Retsch).

Resulting powder was solubilized in 1% digitonin (D1414, SIGMA), 50mM Tris/Cl, 150 mM NaCl, pH 7.5. Proteins were extracted using Monoclonal Anti-HA−Agarose antibody produced in mouse (SIGMA) / GFP-Trap (chromotek) for 1h followed by three washes with 150 mM NaCl, 50 mM Tris HCl pH 7. Bound proteins were released from the beads by a 30 second acidic treatment (0.2M Glycine pH 2.5), which was neutralized with 1M Tris pH 9.4. The eluted proteins were digested with 0.4 µg sequencing grade trypsin for 2h, in the presence of 100 µl of 2 M urea, 50 mM Tris HCl pH 7.5, 1 mM DTT Resulting peptides were acidified with Trifluoroacetic acid (TFA) and purified on C18 StageTips. LC-MS/MS analysis was performed on the EASY-nLC1000 UHPLC (Thermo Scientific) coupled to the Q-Exactive mass spectrometer (Thermo Scientific). Peptides were loaded onto the column with buffer A (0.5% acetic acid) and separated on a 50 cm PepMap column (75 µm i.d. 2 µm beads; Dionex) using a 4 h gradient of 5-30% buffer B (80% acetonitrile, 0.5% acetic acid). Interactors were extracted by comparing the protein intensities to a wild type (BY4741) control.

Western blot analysis

Yeast proteins were extracted either by NaOH or TCA protocol as previously described[59] and resolved on polyacrylamide gels, transferred to nitrocellulose membranes blots, and probed with primary rabbit/mouse antibody against Pma1 (Abcam, ab4645), HA (Covance, MMS-101P) or GFP (Abcam, ab290). The membranes were then probed with a secondary goat-anti-rabbit/mouse antibody conjugated to IRDye800 or to IRDye680 (LI-COR Biosciences). Membranes were scanned for infrared signal using the Odyssey Imaging System.

Blue native gel electrophoresis

Yeast microsomes were prepared according to[60]. In brief, spheroplasts of yeast were lysed by dounce homogenisation (25 strokes) in lysis buffer (0.1 M Sorbitol, 20 mM HEPES pH 7.4, 50 mM Potassium acetate, 2 mM EDTA, 1 mM DTT, 1 mM PMSF) at 4°C. The lysates were centrifuged at 1000g and the resulting supernatant at 27,000g for 10 min at 4°C. The crude membrane pellet was re-suspended in lysis buffer and layered onto a discontinuous sucrose density gradient consisting of 1.2 and 1.5 M sucrose. Following centrifugation at 100,000g for 60 min at 4°C the membranes at the 1.2-1.5 M sucrose interface were collected and washed twice in lysis buffer. The membrane pellets were re-supended in membrane storage buffer (50 mM Nacl, 0.32 M sucrose, 20 mM HEPES pH 7.4, 2 mM EDTA containing protease inhibitors) and the protein concentration determined by a standard Bradford assay[60].

Microsomes were solubilised in ComplexioLyte 48 buffer (1mg/ml, Logopharm) for 30 min at 4°C (2). Solubilised extracts were centrifuged at 100,000g for 30 min at 4°C and supplemented with glycerol (5%) and Coomassie G-250 (0.3%) and loaded on a 3.5 - 15% linear native polyacrylamide gel. The BN-PAGE gel was prepared according to[61]. The gel buffer contained 25 mM imidazole and 500 mM 6-Aminohexanoic acid. The cathode chamber was first filled with cathode buffer B (50 mM Tricine, 7.5 mM imidazole and 0.02% coomassie) and subsequently replaced by cathode buffer B/10 (containing 0.002% coomassie) after the gel running front had covered a third of the desired distance of electrophoresis. The anode chamber was filled with 25 mM imidazole, pH 7.0. A high molecular weight calibration kit for native electrophoresis from GE Healthcare was used as a standard[61,62].

ACKNOWLEDGEMENTS

This work was supported by a BSF collaborative grant to Elizabeth Miller and Maya Schuldiner (2013101) as well as a grant by the Deutsche Forschungsgemeinschaft (SFB1190; Compartmental Gates and Contact Sites) to Maya Schuldiner (P11) and Blanche Schwappach (P04) and the Prof. Rami Rahamimoff BSF travel grant to Yosef Geva T-2014-130. Work in the Miller lab was also supported by the US National Institutes of Health under award number R01GM085089 and in the UK by the Medical Research Council (MC_UP_1201/10). We thank Jim Haber for fruitful discussions. Maya Schuldiner is an Incumbent of the Dr. Gilbert Omenn and Martha Darling Professorial Chair in Molecular Genetics.

FIGURE LEGENDS

Figure 1: A systematic approach identifies a potential new cargo receptor

(A) To uncover new cargo receptors we integrated mutations in *sec24-A* or *C* cargo-binding sites into every strain of the yeast secretome-GFP collection. We then followed the localization of each protein by high-content screening and manual comparison between the mutated and the control strains. (B) The mutation in the *sec24-C* binding site resulted in localization changes of four cargo receptors of the p24 protein family. The cargo receptors alter their localization from ER in the control cells (*SEC24* wild type) to punctate localization in the mutant (*sec24-C*). (C) Most proteins did not change localization as a result of mutations in *sec24-A* or *C* cargo-binding sites compared to the control (*sec24-A/C*/wild type respectively). Dpl1 is an example for such a protein. Three proteins changed their localization from ER to punctate pattern in both mutants: Erd2, Erv41 and Ydl121c. Bar=5µ

Figure 2: Genetic and physical interactions of

Ydl121c suggest Pma1 as a possible cargo protein.

(A) Schematic of the predicted topology of Ydl121c. (B) Ydl121c-HA is packaged into COPII vesicles. Microsomal membranes were incubated with COPII proteins and GTP (+) or GDP (−), vesicle fractions were separated from total membranes (T) and detected by immunoblotting with αHA / αErv41 antibodies. Erv41 served as a positive control for vesicle formation. (C) Affinity precipitation of HA-tagged Ydl121c followed by mass spectrometry revealed Ydl121c physical interactors and suggests Pma1 as its possible cargo. The table shows all proteins enriched more than four fold in the sample compared to control (WT cells). (D) Tetrad anlysis of ascospores resulting from meiosis of [*ydl121c*+/-*lst1*+/-] diploids reveales synthetic lethality between the two genes. *Δydl121c* strain is $G418^R$ and *Δlst1* strain is Nat^R.

Figure 3: *YDL121C* and *LST1* have parallel roles.

(A) *YDL121C* and *LST1* show similar genetic interactions with *SEC13*. Strains containing deletions in *ydl121c* or *lst1* on the background of the temperature sensitive mutation *sec13-1* were spotted as serial dilutions onto media containing 5-FOA to counter-select for the *SEC13-URA3* plasmid and test viability in restrictive temperatures. On standard media (left panels), all strains grew uniformly. In the absence of *SEC13* (5FOA, right panels) *Δydl121c* or *Δlst1* were both synthetic sick. Overexpression (O.E) of *YDL121C* was able to rescue the deletion of *lst1*. Native or over expression of *LST1* could not rescue the deletion of *ydl121c.* (B) *YDL121C* overexpression (O.E) can rescue *Δlst1* growth delay on low pH. *Δlst1* strains were grown in different pH levels. The known growth delay phenotype of *Δlst1* in low pH was rescued by native expression of LST1 and O.E of *YDL121C* to the same extent. (C) *Δydl121c* does not affect trafficking of Gas1 (another Lst1-dependent substrate). Pulse-chase maturation experiment following Gas1 maturation over time demonstrates that *Δlst1* but not *Δydl121c* affects the export rate from the ER (seen by glycosylation states: m-mature p-premature) of Gas1. (n = 3, mean ± SD).

Figure 4: Ykl077w is an uncharacterized binding partner of Ydl121c.

(A) Schematic of the predicted structure of Ykl077w. Red circles represent the predicted signal peptide, blue circles represent predicated retrieval motifs, red asterisk indicates the Kex2 cleavage site. (B) Ykl077w cleavage by Kex2 gives rise to two products of proteolytic processing: YKl077w-N' and Ykl077w-C'. The Kex2-dependent size-shift was visualized by western blotting in control (WT) or Δ*kex2* strains for either C' tagged Ykl077w or N' tagged Ykl077w under control of their native promoter. The full length protein is ~64kD. Ykl077w-N' is ~ 46 kD and Ykl077w-C' is ~18kD. For further details see Fig S2 (C) Ykl077w-N' co-localized mainly with the mid Golgi marker, Mnn9, and is also present in the ER (which could be the unprocessed form) (D) Ykl077w-C' mainly co-localizes with a COPI marker. Some coloclization was also observed with Golgi markers. Bar=5μ

Figure 5: Ydl121c and Ykl077w are essential for optimal Pma1 maturation. (A) Left: Protein extraction and separation on SDS-PAGE shows that Ydl121c and Ykl077w affect Pma1 levels. Right: Comassie staining of the membrane shows no change in general protein abundance. Bottom: Quantification of Pma1 signal relative to two other membrane proteins (Sso1/2 or Sec61) shows specific reduction of more than 20% in Pma1 abundance on the background of Δ*ydl121c* and more than 80% on the background of Δ*ykl077w*. (n = 6, mean ± SE). (B) Ydl121c and Ykl077w affect the abundance of Pma1 oligomers. Protein extraction and separation on Blue Native (BN)-PAGE show reduction in Pma1 abundance on the background of Δ*ydl121c* and Δ*ykl077w* in all oligomeric states. Arowheads indicate different multimeric states of Pma1. assignment of stoichiometries was done according to[40,46]. (C) Ydl121c and Ykl077w affect Pma1 localization at steady state. After 72 hours of continuous growth in logarithmic phase, maintained by consistent dilution of the culture, Pma1 showed ER retention on the background of Δ*ydl121c* (quantification shown in upper left corner of images) and much stronger vacuolar staining on the background of Δ*ykl077w*. (D) Quantification of Western blot detecting both Pma1-GFP and free GFP (using anti-GFP antibodies) on the backround of Δ*ydl121c and* Δ*ykl077w*. Calculation of free GFP/ Pma1-GFP ratio shows 30% higher abundance of free GFP on the background of Δ*ykl077w* relative to control strain. (n = 3, mean ± SE).

Figure 6: A schematic model of the roles of Ydl121c (Exp1) and Ykl077w (Psg1) in Pma1 sorting and maturation.

Based on our observations we suggest that Ydl121c (from hereon called Exp1) is a Pma1 cargo receptor. Since it can promote ER to Golgi traffic independently of Lst1 we conclude that it is not essential for Pma1 trafficking through COPII vesicles constructed of Sec24 and Lst1 isoforms but rather that it is esential in vesicles constructed of Sec24 proteins only. This suggests that there exist two, parallel, routes to enable Pma1 exit.

Ykl077w (from hereon called Psg1) is cleaved giving rise to two cleavage products: Ykl077w-N' (Psg1-N') that is localized mainly to the ER and mid Golgi and Ykl077w-C' (Psg1-C') localized mainly to COPI vesicles. Deletion of the complete gene causes instability of Pma1 and enhanced vacuolar

degradation. Considering it's localization and deletion phenotype yet lack of physical interaction with Pma1, we suggest that Ykl077w might have an indirect role in retrieval of immature Pma1 from the Golgi back to the ER or in promoting its maturation in the Golgi.

Table S1: Yeast strains used in this paper

Table S2: Plasmids used in this paper

Table S3: Strains in the GFP secretome library

Table S4*: YDL121C* synthetic lethal interactions

Five most consistent Δ*ydl121c* synthetic lethal interactors from a whole-genome synthetic lethality screen. The first two are *LST1,* the *SEC24* homolog with a specific role in Pma1 ER-to-Golgi traffic and *BRP1* a gene located in the upstream region of *PMA1* whose deletion creates a hypomorphic allele of *PMA1*.

Table S5: N' GFP-Ykl077w physical interactors

Most enriched proteins identified in affinity precipitation of GFP-Ykl077w followed by mass spectrometry. The table shows all proteins enriched more than four fold in the sample compared to control (Cells expressing cytosolic GFP).

Table S6: C' Ykl077w-GFP physical interactors

Most enriched proteins identifeied in affinity precipitation of Ykl077w-GFP followed by mass spectrometry. The table shows all proteins enriched more than four fold in the sample compared to the control (Cells expressing cytosolic GFP).

Figure S1: Ydl121c-GFP co-localizes with COPI markers on the background of sec24-A or C mutants.

Co-expression of Ydl121c-GFP on the background of *sec24* mutations with mCherry tagged markers for COPI, COPII or Golgi (Cop1, Sec13 and Vrg4 respectivly) show best co-localization with the COPI marker. Bar=5μ.

Figure S2: Parameters affecting Ykl077w-N'/C' size

(A) Residues of Ykl077w shown to be O-mannosylated in a high throughput analysis of glycosylation in yeast [44]. Blue letters indicate the O-mannosylation sites, Orange- signal peptide, purple-transmembrane domain and red- Kex2 cleavage site. (B) Calculation of Ykl077w-N'/C' sizes as assayed by Western blot.

Figure S3: Microscopy and western blot analysis of Pma1-GFP in *Δykl077w* and *Δmnn11* single and double mutants.

Δ*mnn11* and Δ*ykl077w* buffer each others enhanced Pma1 degradation phenotype. After 72 hours of continuous growth in logarithmic phase, maintained by consistent dilution of the culture, Pma1 showed strong vacuolar staining on the background of *Δmnn11* or Δ*ykl077w*. Bar=5μ However, double deletion *Δmnn11*/Δ*ykl077w* rescued this phenotype. Moreover, the ratio of free GFP/Pma1-GFP as assayed by Western blot was similar to WT in the double deletion strain, suggesting reduced vacoular degradation of Pma1 relative to each single mutant. N=3 bar=±SE.

REFERENCES

1. Barlowe C, Orci L, Yeung T. COPII: A Membrane Coat Formed by Set Proteins That Drive Vesicle Budding from the Endoplasmic Reticulum. *Cell*. 1994;77.
2. Thor F, Gautschi M, Geiger R, Helenius A. Bulk flow revisited: transport of a soluble protein in the secretory pathway. *Traffic*. 2009;10:1819-1830.
3. Barlowe C, Helenius A. Cargo Capture and Bulk Flow in the Early Secretory Pathway. *Annu Rev Cell Dev Biol*. 2016;32:197-222.
4. Nickel W, Brügger B, Wieland FT. Vesicular transport: the core machinery of COPI recruitment and budding. *J Cell Sci*. 2002;115:3235-3240.
5. Dancourt J, Barlowe C. Protein sorting receptors in the early secretory pathway. *Annu Rev Biochem*. 2010;79:777-802.
6. Mossessova E, Bickford LC, Goldberg J. SNARE selectivity of the COPII coat. *Cell*. 2003;114:483-495.
7. Miller E a, Beilharz TH, Malkus PN, et al. Multiple cargo binding sites on the COPII subunit Sec24p ensure capture of diverse membrane proteins into transport vesicles. *Cell*. 2003;114:497-509.
8. Pagant S, Wu A, Edwards S, Diehl F, Miller EA. Sec24 Is a Coincidence Detector that Simultaneously Binds Two Signals to Drive ER Export. *Curr Biol*. 2015;25:403-412.
9. Shimoni Y, Kurihara T, Ravazzola M, Amherdt M, Orci L, Schekman R. Lst1p and Sec24p cooperate in sorting of the plasma membrane ATPase into COPII vesicles in Saccharomyces cerevisiae. *J Cell Biol*. 2000;151:973-984.
10. Miller E, Antonny B, Hamamoto S, Schekman R. Cargo selection into COPII vesicles is driven by the Sec24p subunit. *EMBO J*. 2002;21:6105-6113.
11. Castillon G a, Aguilera-Romero A, Manzano-Lopez J, et al. The yeast p24 complex regulates GPI-anchored protein transport and quality control by monitoring anchor remodeling. *Mol Biol Cell*. 2011;22:2924-2936.
12. Roberg KJ, Crotwell M, Espenshade P,

Gimeno R, Kaiser C a. LST1 is a SEC24 homologue used for selective export of the plasma membrane ATPase from the endoplasmic reticulum. *J Cell Biol*. 1999;145:659-672.

13. Gillon AD, Latham CF, Miller E a. Vesicle-mediated ER export of proteins and lipids. *Biochim Biophys Acta - Mol Cell Biol Lipids*. 2012;1821:1040-1049.

14. Belden WJ, Barlowe C. Role of Erv29p in collecting soluble secretory proteins into ER-derived transport vesicles. *Science*. 2001;294(5546):1528-1531. doi:10.1126/science.1065224.

15. Belden, W ; Barlowe C. Erv25p, a Component of COPII-coated Vesicles, Forms a Complex with Emp24p That Is Required for Efficient Endoplasmic Reticulum to Golgi Transport. *J Biol Chem*. 1996;271:26939-26946.

16. Belden WJ, Barlowe C. Distinct roles for the cytoplasmic tail sequences of Emp24p and Erv25p in transport between the endoplasmic reticulum and Golgi complex. *J Biol Chem*. 2001;276:43040-43048.

17. Geva Y, Schuldiner M. The back and forth of cargo exit from the endoplasmic reticulum. *Curr Biol*. 2014;24:R130-R136.

18. Powers J, Barlowe C. Erv14p Directs a Transmembrane Secretory Protein into COPII-coated Transport Vesicles. 2002;13:880-891.

19. Herzig Y, Sharpe HJ, Elbaz Y, Munro S, Schuldiner M. A systematic approach to pair secretory cargo receptors with their cargo suggests a mechanism for cargo selection by Erv14. *PLoS Biol*. 2012;10:e1001329.

20. Bue C, Barlowe C. Molecular dissection of Erv26p identifies separable cargo binding and coat protein sorting activities. *J Biol Chem*. 2009; 284:24049–60

21. Noda Y, Yoda K. Svp26 facilitates endoplasmic reticulum to Golgi transport of a set of mannosyltransferases in Saccharomyces cerevisiae. *J Biol Chem*. 2010; 285:15420-9

22. Zhang B, Cunningham M a, Nichols WC, et al. Bleeding due to disruption of a cargo-specific ER-to-Golgi transport complex. *Nat Genet*. 2003;34:220-225.

23. Cortini M, Sitia R. ERp44 and ERGIC-53 synergize in coupling efficiency and fidelity of IgM polymerization and secretion. *Traffic*. 2010;11:651-659.

24. Margulis NG, Wilson JD, Bentivoglio CM, Dhungel N, Gitler AD, Barlowe C. Analysis of COPII vesicles indicates a role for the Emp47-Ssp120 complex in transport of cell surface glycoproteins. *Traffic*. 2015;1:191-210.

25. Huh W-K, Falvo J, Huh W-K, et al. Global analysis of protein localization in budding yeast. *Nature*. 2003;425(6959):686-691.

26. Miller EA, Liu Y, Barlowe C, Schekman R. ER-Golgi transport defects are associated with mutations in the Sed5p-binding domain of the COPII coat subunit, Sec24p. *Mol Biol Cell*. 2005;16(8):3719-3726.

27. Cohen Y, Schuldiner M. Advanced methods for high-throughput microscopy screening of genetically modified yeast libraries. *Methods Mol Biol*. 2011;781:127-159.

28. Breker M, Gymrek M, Schuldiner M. A novel single-cell screening platform reveals proteome plasticity during yeast stress responses. *J Cell Biol*. 2013;200:839-850.

29. Semenza JC, Hardwick KG, Dean N, Pelham HRB. ERD2, a yeast gene required for the receptor-mediated retrieval of luminal ER proteins from the secretory pathway. *Cell*. 1990;61:1349-1357.

30. Shibuya a., Margulis N, Christiano R, Walther TC, Barlowe C. The Erv41-Erv46 complex serves as a retrograde receptor to retrieve escaped ER proteins. *J Cell Biol*. 2015; 208:197-209.

31. Käll L, Krogh A, Sonnhammer ELL. Advantages of combined transmembrane topology and signal peptide prediction-the Phobius web server. *Nucleic Acids Res*. 2007;35:429-432.

32. Omasits U, Ahrens CH, Müller S, Wollscheid B. Protter: Interactive protein feature visualization and integration with experimental proteomic data. *Bioinformatics*. 2014;30:884-886.

33. Aviram N, Schuldiner M. Embracing the void-how much do we really know about targeting and translocation to the endoplasmic reticulum? *Curr Opin Cell Biol*. 2014;29:8-17.

34. Aviram N, Ast T, Costa EA, et al. The SND proteins constitute an alternative targeting route to the endoplasmic reticulum. *Nature*. 2016;540:134-138.

35. Giaever G, Chu AM, Ni L, et al. Functional profiling of the Saccharomyces cerevisiae genome. *Nature*. 2002;418:387-391.

36. Breslow DK, Cameron DM, Collins SR, et al. A comprehensive strategy enabling high-resolution functional analysis of the yeast genome. *Nat Methods*. 2008;5:711-718.

37. Porat Z, Wender N, Erez O, Kahana C. Mechanism of polyamine tolerance in yeast :

novel regulators and insights. 2005;62:3106-3116.

38. Aouida M, Leduc A, Poulin R, Ramotar D. AGP2 Encodes the Major Permease for High Affinity Polyamine Import in Saccharomyces cerevisiae. 2005;280:24267-24276.

39. Ambesi a, Miranda M, Petrov V V, Slayman CW. Biogenesis and function of the yeast plasma-membrane H(+)-ATPase. *J Exp Biol*. 2000;203:155-160.

40. Lee MCS, Hamamoto S, Schekman R. Ceramide biosynthesis is required for the formation of the oligomeric H+-ATPase Pma1p in the yeast endoplasmic reticulum. *J Biol Chem*. 2002;277:22395-22401.

41. Tarassov K, Messier V, Landry CR, et al. An in vivo map of the yeast protein interactome. *Science*. 2008;320:1465-1470.

42. Heiman MG, Engel A, Walter P. The Golgi-resident protease Kex2 acts in conjunction with Prm1 to facilitate cell fusion during yeast mating. *J Cell Biol*. 2007;176:209-22.

43. Wächter A, Schwappach B. The yeast CLC chloride channel is proteolytically processed by the furin-like protease Kex2p in the first extracellular loop. *FEBS Lett*. 2005;579:1149-1153.

44. Neubert P, Halim A, Zauser M, et al. Mapping the O-Mannose Glycoproteome in Saccharomyces cerevisiae. *Mol Cell Proteomics*. 2016;15:1323-1337.

45. Koh JLY, Ding H, Costanzo M, et al. DRYGIN: a database of quantitative genetic interaction networks in yeast. *Nucleic Acids Res*. 2010;38:D502-7.

46. Eraso P, Mazón MJ, Portillo F. A dominant negative mutant of PMA1 interferes with the folding of the wild type enzyme. *Traffic*. 2010;11:37-47.

47. Nikko E, Pelham HRB. Arrestin-mediated endocytosis of yeast plasma membrane transporters. *Traffic*. 2009;10:1856-1867.

48. Chang a., Fink GR. Targeting of the yeast plasma membrane [H+]ATPase: A novel gene AST1 prevents mislocalization of mutant ATPase to the vacuole. *J Cell Biol*. 1995;128:39-49.

49. Bagnat M, Chang a, Simons K. Plasma membrane proton ATPase Pma1p requires raft association for surface delivery in yeast. *Mol Biol Cell*. 2001;12(12):4129-4138.

50. Ding J, Segarra VA, Chen S, Cai H, Lemmon SK, Ferro-Novick S. Auxilin facilitates membrane traffic in the early secretory pathway. *Mol Biol Cell*. 2015;27:127-136.

51. Sato M, Sato K, Nakano A. Endoplasmic reticulum quality control of unassembled iron transporter depends on Rer1p-mediated retrieval from the golgi. *Mol Biol Cell*. 2004;15:1417-1424.

52. Wang Q, Chang A. Substrate recognition in ER-associated degradation mediated by Eps1, a member of the protein disulfide isomerase family. *EMBO J*. 2003;22:3792-3802.

53. Brachmann CB, Davies A, Cost GJ, et al. Designer deletion strains derived from Saccharomyces cerevisiae S288C: a useful set of strains and plasmids for PCR-mediated gene disruption and other applications. *Yeast*. 1998;14:115-132.

54. Daniel Gietz R, Woods RA. *Guide to Yeast Genetics and Molecular and Cell Biology - Part B*. Vol 350. Elsevier; 2002.

55. Yofe I, Schuldiner M. Primers-4-Yeast: a comprehensive web tool for planning primers for Saccharomyces cerevisiae. *Yeast*. 2014;31:77-80.

56. Goldstein AL, McCusker JH. Three new dominant drug resistance cassettes for gene disruption inSaccharomyces cerevisiae. *Yeast*. 1999;15:1541-1553.

57. Hanscho M, Ruckerbauer DE, Chauhan N, et al. Nutritional requirements of the BY series of Saccharomyces cerevisiae strains for optimum growth. *FEMS Yeast Res*. 2012;12:796-808.

58. D'Arcangelo JG, Crissman J, Pagant S, et al. Traffic of p24 Proteins and COPII Coat Composition Mutually Influence Membrane Scaffolding. *Curr Biol*. 2015;25:1296-1305.

59. Ast T, Cohen G, Schuldiner M. A network of cytosolic factors targets SRP-independent proteins to the endoplasmic reticulum. *Cell*. 2013;152:1134-1145.

60. Wuestehube LJ, Schekman RW. Reconstitution of transport from endoplasmic reticulum to golgi complex using endoplasmic reticulum-enriched membrane fraction from yeast. *Methods Enzymol*. 1992;219:124-136.

61. Wittig I, Braun H-P, Schägger H. Blue native PAGE. *Nat Protoc*. 2006;1:418-428.

62. Schwenk J, Harmel N, Zolles G, et al. Functional proteomics identify cornichon proteins as auxiliary subunits of AMPA receptors. *Science*. 2009;323:1313-1319.

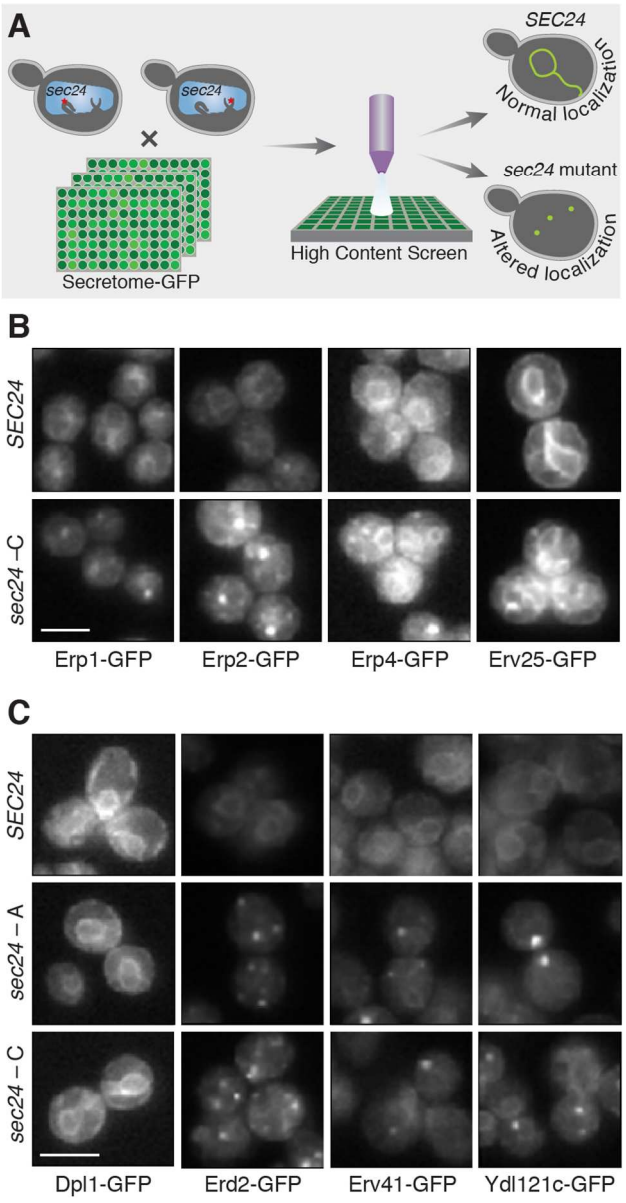

Figure 1: A systematic approach identifies a potential new cargo receptor
(A) To uncover new cargo receptors we integrated mutations in sec24-A or C cargo-binding sites into every strain of the yeast secretome-GFP collection. We then followed the localization of each protein by high-content screening and manual comparison between the mutated and the control strains. (B) The mutation in the sec24-C binding site resulted in localization changes of four cargo receptors of the p24 protein family. The cargo receptors alter their localization from ER in the control cells (SEC24 wild type) to punctate localization in the mutant (sec24-C). (C) Most proteins did not change localization as a result of mutations in sec24-A or C cargo-binding sites compared to the control (sec24-A/C/wild type respectively). Dpl1 is an example for such a protein. Three proteins changed their localization from ER to punctate pattern in both mutants: Erd2, Erv41 and Ydl121c. Bar=5μ

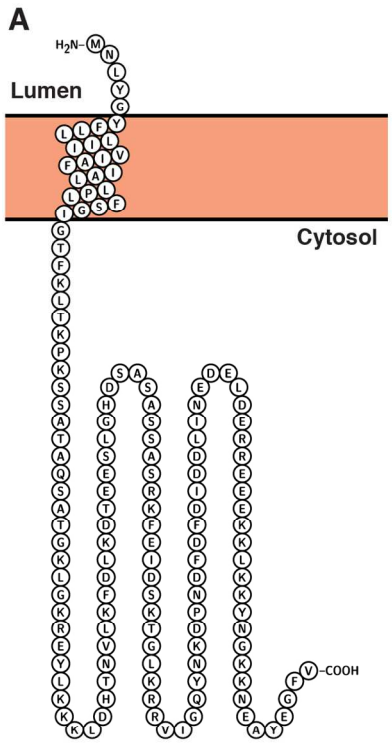

C

Proteins that co-immunoprecipitate with Ydl121c-HA		
Protein	**Localization**	**Average fold change from W.T**
Sec72	Translocon	infinite
Snd3	Translocon	infinite
Cys4	Cytoplasm	infinite
Erv14	COPII	infinite
Hsc82	Cytoplasm	infinite
Sec28	COPI	infinite
Hsp60	Mitochondria	infinite
Ydl121c	ER	12.4
Pma1	Plasma membrane	7.7
Por1	Mitochondria	7.7
Sss1	Translocon	7.4
Sec63	Translocon	4.8

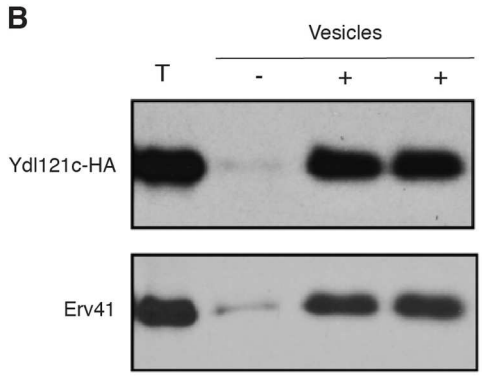

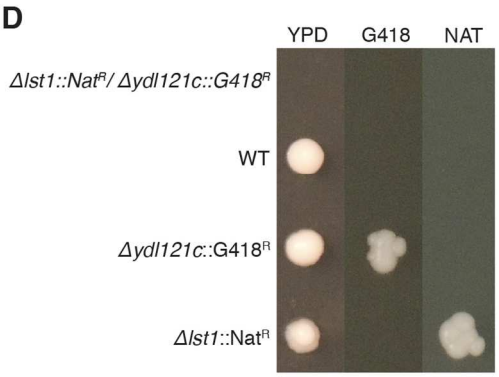

Figure 2: Genetic and physical interactions of Ydl121c suggest Pma1 as a possible cargo protein. (A) Schematic of the predicted topology of Ydl121c. (B) Ydl121c-HA is packaged into COPII vesicles. Microsomal membranes were incubated with COPII proteins and GTP (+) or GDP (−), vesicle fractions were separated from total membranes (T) and detected by immunoblotting with αHA / αErv41 antibodies. Erv41 served as a positive control for vesicle formation. (C) Affinity precipitation of HA-tagged Ydl121c followed by mass spectrometry revealed Ydl121c physical interactors and suggests Pma1 as its possible cargo. The table shows all proteins enriched more than four fold in the sample compared to control (WT cells). (D) Tetrad anlysis of ascospores resulting from meiosis of [ydl121c+/- lst1+/-] diploids reveales synthetic lethality between the two genes. Δydl121c strain is $G418^R$ and Δlst1 strain is Nat^R.

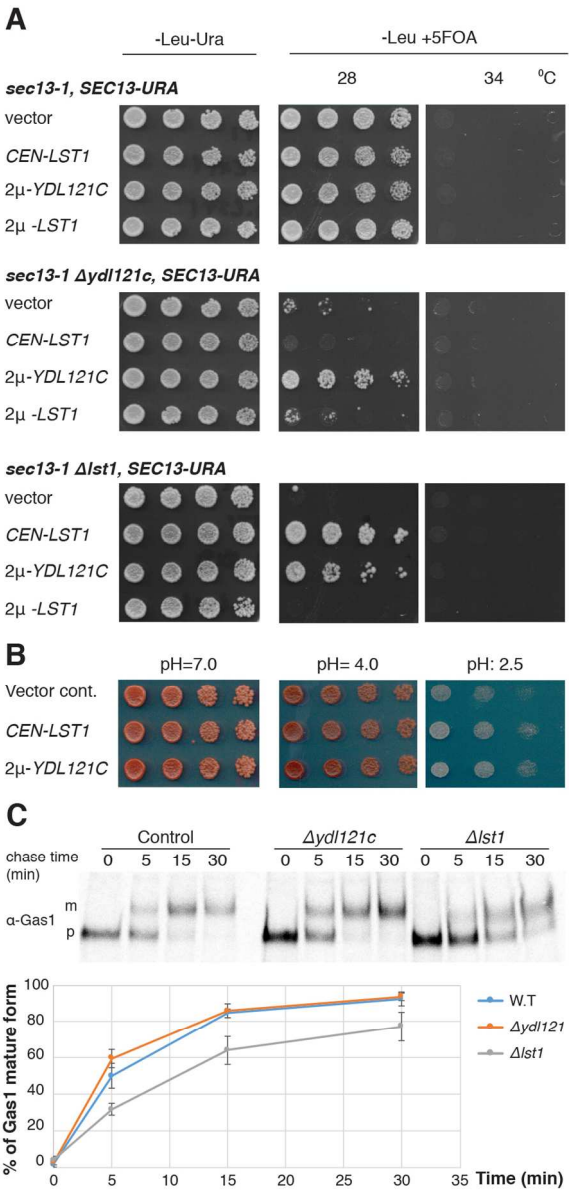

Figure 3: YDL121C and LST1 have parallel roles.
(A) YDL121C and LST1 show similar genetic interactions with SEC13. Strains containing deletions in ydl121c or lst1 on the background of the temperature sensitive mutation sec13-1 were spotted as serial dilutions onto media containing 5-FOA to counter-select for the SEC13-URA3 plasmid and test viability in restrictive temperatures. On standard media (left panels), all strains grew uniformly. In the absence of SEC13 (5FOA, right panels) Δydl121c or Δlst1 were both synthetic sick. Overexpression (O.E) of YDL121C was able to rescue the deletion of lst1. Native or over expression of LST1 could not rescue the deletion of ydl121c. (B) YDL121C overexpression (O.E) can rescue Δlst1 growth delay on low pH. Δlst1 strains were grown in different pH levels. The known growth delay phenotype of Δlst1 in low pH was rescued by native expression of LST1 and O.E of YDL121C to the same extent. (C) Δydl121c does not affect trafficking of Gas1 (another Lst1-dependent substrate). Pulse-chase maturation experiment following Gas1 maturation over time demonstrates that Δlst1 but not Δydl121c affects the export rate from the ER (seen by glycosylation states: m-mature p-premature) of Gas1. (n = 3, mean ± SD).

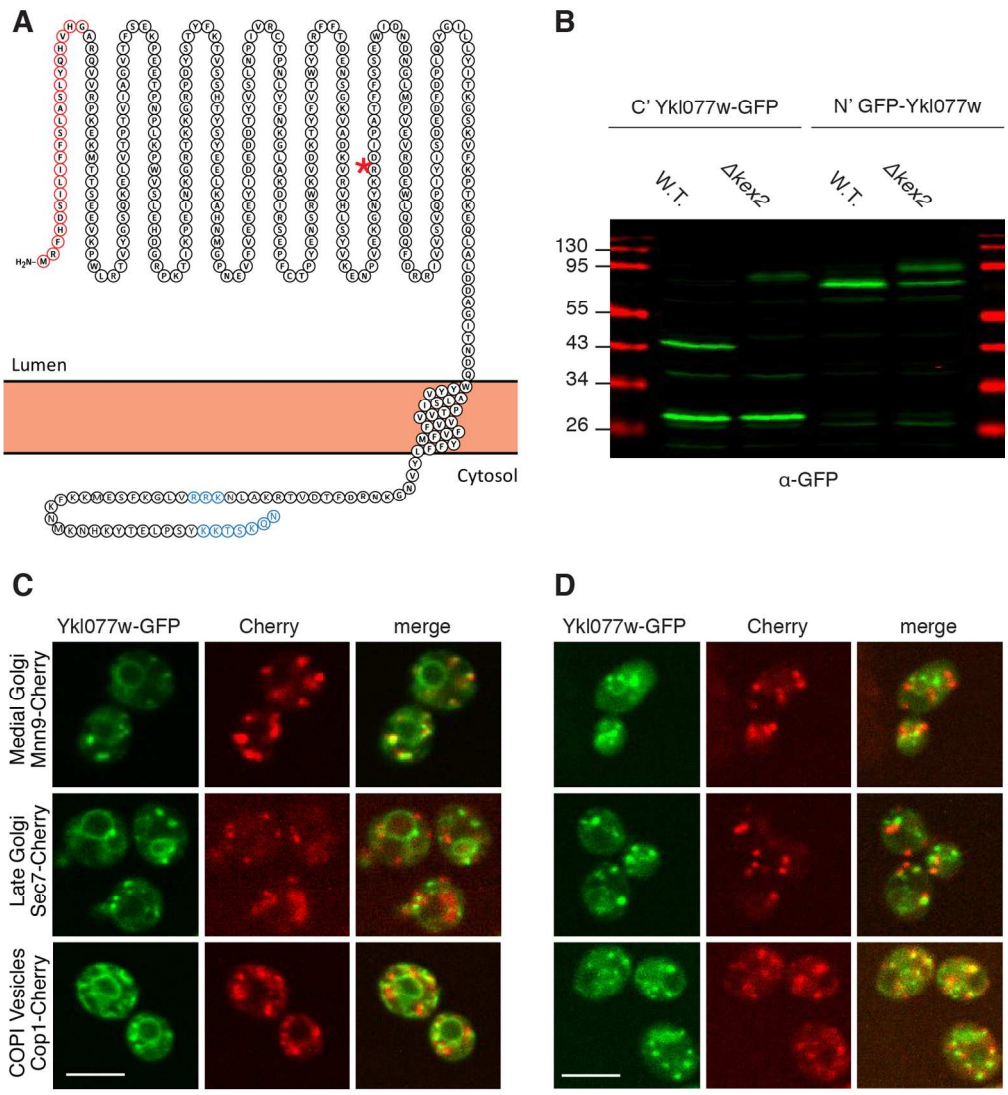

Figure 4: Ykl077w is an uncharacterized binding partner of Ydl121c.
(A) Schematic of the predicted structure of Ykl077w. Red circles represent the predicted signal peptide, blue circles represent predicated retrieval motifs, red asterisk indicates the Kex2 cleavage site. (B) Ykl077w cleavage by Kex2 gives rise to two products of proteolytic processing: YKl077w-N' and Ykl077w-C'. The Kex2-dependent size-shift was visualized by western blotting in control (WT) or Δkex2 strains for either C' tagged Ykl077w or N' tagged Ykl077w under control of their native promoter. The full length protein is ~64kD. Ykl077w-N' is ~46 kD and Ykl077w-C' is ~18kD. For further details see Fig S2 (C) Ykl077w-N' co-localized mainly with the mid Golgi marker, Mnn9, and is also present in the ER (which could be the unprocessed form) (D) Ykl077w-C' mainly co-localizes with a COPI marker. Some coloclization was also observed with Golgi markers. Bar=5μ

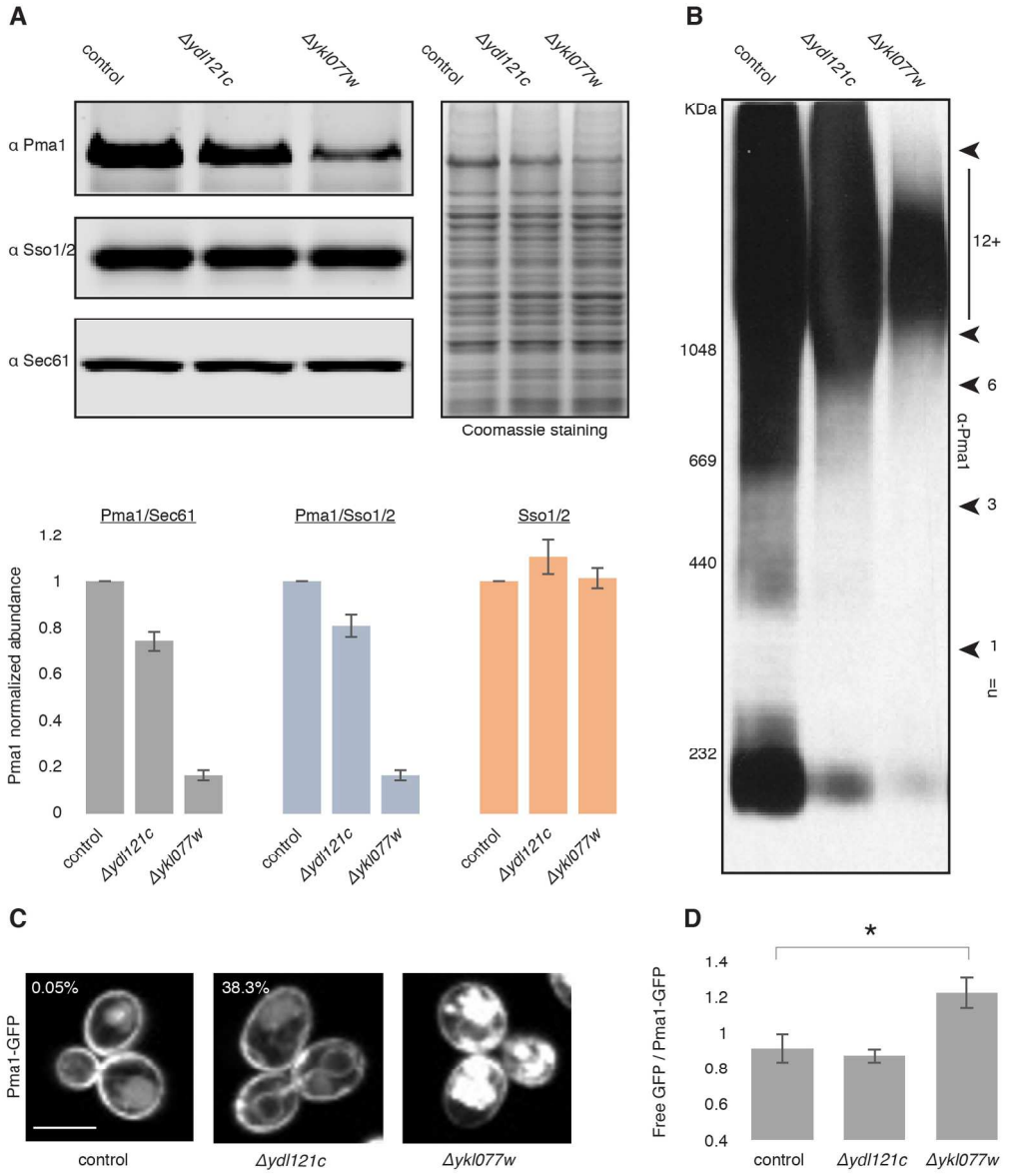

Figure 5: Ydl121c and Ykl077w are essential for optimal Pma1 maturation. (A) Left: Protein extraction and separation on SDS-PAGE shows that Ydl121c and Ykl077w affect Pma1 levels. Right: Comassie staining of the membrane shows no change in general protein abundance. Bottom: Quantification of Pma1 signal relative to two other membrane proteins (Sso1/2 or Sec61) shows specific reduction of more than 20% in Pma1 abundance on the background of Δydl121c and more than 80% on the background of Δykl077w. (n = 6, mean ± SE). (B) Ydl121c and Ykl077w affect the abundance of Pma1 oligomers. Protein extraction and separation on Blue Native (BN)-PAGE show reduction in Pma1 abundance on the background of Δydl121c and Δykl077w in all oligomeric states. Arrowheads indicate different multimeric states of Pma1. assignment of stoichiometries was done according to40,46. (C) Ydl121c and Ykl077w affect Pma1 localization at steady state. After 72 hours of continuous growth in logarithmic phase, maintained by consistent dilution of the culture, Pma1 showed ER retention on the background of Δydl121c (quantification shown in upper left corner of images) and much stronger vacuolar staining on the background of Δykl077w. Bar= 5μ. (D) Quantification of Western blot detecting both Pma1-GFP and free GFP (using anti-GFP antibodies) on the backround of Δydl121c and Δykl077w. Calculation of free GFP/ Pma1-GFP ratio shows 30% higher

abundance of free GFP on the background of Δykl077w relative to control strain. (n = 3, mean ± SE).

168x198mm (300 x 300 DPI)